Figure 2 shows the results of the calculations with flow values, pressure ratio, and total temperature plotted over the nozzle length. The segment size had been reduced in these calculations to the point where its influence on the results practically disappeared. The supersonic Mach number curve demonstrates the influence of the segment size, comparing it also with the condition encountered with the method of Ref. 1. If the segment size for both methods is reduced to the point of no influence, complete agreement exists between both methods. However, the segment size required by the method of Ref. 1 is about five times smaller than that required for the present method; i.e., for the same accuracy, the method of Ref. 1 requires many more steps in the calculation than the present method. By increasing the segment size for the present method by a factor of five, the solid points above the Mach number curve in Fig. 2 result. By using the same segment size for the method of Ref. 1, the Mach numbers marked by the crosses above the solid points are obtained; i.e., for the same enlarged segment size the method of Ref. 1 deviates much more from accurate values than the present method.

The present method has another advantage. It does not become undetermined at Mach 1, as evident from Eq. (13); i.e., no special precautions are necesary for supersonic calculations near the sonic point [for subsonic calculations, inadmissable segment area ratios recognized by imaginary results in Eq. (14) must be avoided].

The flow process least accessible to the present calculation method is subsonic diffusion. In this process, unpredictable flow separation is likely to occur, which, in general, makes a fair estimate of τ very difficult.

References

[1] Shapiro, A. H., *The Dynamics and Thermodynamics of Compressible Fluid Flow*, Vol. 1, The Ronald Press Co., New York, 1953, p. 219.

[2] Hasinger, S. H., "Performance Characteristics of Ejector Devices," Aerospace Research Laboratories, ARL TR-75-0205, WP AFB, Ohio, June 1975.

[3] Hasinger, S. H., "Ejector Optimization," AFFDL-TR-78-23, WP AFB, Ohio, June 1978.

Wall Mass Transfer and Pressure Gradient Effects on Turbulent Skin Friction

Ralph D. Watson* and R. Balasubramanian†
NASA Langley Research Center, Hampton, Virginia

Introduction

MOTIVATED by current research on viscous drag reduction, the effects of mass injection and pressure gradients on the drag of surfaces were examined theoretically using boundary-layer and Navier-Stokes codes. Two turbulent flow cases were considered: the effect of spatially nonuniform surface injection with fixed total mass flow rate on a flat surface, and the effect of sinusoidal mass injection and suction on a sinusoidal surface in the presence of a streamwise pressure gradient. For a flat surface the skin friction reduction due to continuous injection is well known; the present study focuses on the effect of spatially varying the injection on flat-plate drag. Little is known regarding the effects of suction and injection on wavy wall surfaces; the present study is also focused on this problem.

Received June 23, 1982; revision received March 1, 1983. This paper is a work of the U.S. Government and therefore is in the public domain.

*Aerospace Engineer, Viscous Flow Branch, High-Speed Aerodynamics Division. Member AIAA.

†Presently with Cambridge Hydrodynamics, Inc. Member AIAA.

Calculations were made for 1.2 m long surfaces, one flat and the other sinusoidal with a wavelength of 30.5 cm. In each case the undisturbed velocity was 15.24 m/s and the initial boundary layer was turbulent at a momentum thickness Reynolds number of 4500. For the flat surface, a finite-difference boundary-layer code[1] was used to determine if spatial variations in mass transfer for a fixed toal flow rate could result in enhanced drag reduction. For the sinusoidal surface, calculations were made with a Navier-Stokes code[2] for a sinusoidal distribution of suction and injection perpendicular to the wall. In both programs mixing length constants of $k=0.41$ and $(\ell/\delta)_{\max}=0.085$ were used in zero-order turbulence closure schemes, and the wall damping factor A^+ was assumed to be the following function of V^+ for low-speed flow[3]:

$$A^+ = 26\exp(-5.9V^+) \tag{1}$$

where $V^+ = v_w/u_\tau$, v = velocity component perpendicular to the wall, and $u_\tau = (\tau_w/\rho)^{1/2}$.

The Navier-Stokes program was checked for coding errors by comparing flat-surface calculations with boundary-layer program calculations for the same input conditions. For no mass transfer the two methods gave essentially the same integrated drag over the 1.2 m surface (see Table 1). Results obtained for an impermeable wall, a flow with constant blowing, and the solution for one cycle of suction and blowing ($v_w/u_\infty=0.005$ at maximum suction and injection) are shown in Fig. 1. The differences in c_f level in the suction portion of the wave can be attributed to the different methods of solution and are considered reasonable by the authors.

Flat Surface Results

Calculations were made using the boundary-layer code to determine the effect of various spatial blowing variations on flat-plate skin friction reduction. Injection was computed for one, two, and four strips, while adjusting the injection rates to keep the total injected mass constant. A uniform blowing rate of $v_w/u_\infty=0.001$ over the complete surface defined the total mass injected. That is, values of v_w/u_∞ equal to 0.002, 0.004, and 0.008 were injected over one-half, one-quarter, and one-eighth surface lengths for single-, double-, and quadruple-step injections, respectively. The drag on the 1.3 m (4 ft) long surface element was obtained by integrating the local skin friction coefficient. (No "correction" or accounting was included for the losses associated with collecting and ducting the air. These losses are a function of the injection air source, laminar flow control (LFC) suction being a

Table 1 Effect of injection method on flat-surface drag reduction

Injection method	v_w/u_∞	$C_D\times 10^3$	Drag reduction % of no-injection drag
None	0	2.86 (Boundary-layer code)	0
	0	2.81 (Navier-Stokes code)	—
Continuous	0.001	2.26	−21.0
Single step	0.002	2.23	−22.1
	0.004	2.27	−20.6
	0.008	2.32	−18.9
Two step	0.002	2.26	−21.1
	0.004	2.30	−19.6
	0.008	2.35	−18.0
Four step	0.002	2.26	−21.1
	0.004	2.31	−19.2
	0.008	2.35	−18.0

particularly "low-loss" source.) The results are summarized in Table 1 as the percentage reduction in drag over the no-blowing case.

It is evident that multiple injection does not degrade drag reduction over the single-step injection case, although there is a very slight enhancement of drag reduction when the peak injection rate is decreased (i.e., the same amount of mass is injected over a larger area). In no case is the drag significantly different from the case of continuous injection. Evidently, for these flow conditions, the total mass injection determines the overall drag reduction. We conclude, therefore, that the net drag reduction is determined primarily by the total mass injected independent of the mode of injection (continuous or step). This may be of significant importance in the structural design of injection surfaces (i.e., discrete injection geometries may have a lower structural weight compared to a porous surface).

Sinusoidal Surface Results

Also investigated was the effect of combined suction and injection on total drag for a rigid wavy surface. The flow over such a surface (with no wall suction or injection) has associated with it a pressure distribution that is a function of the amplitude of the wave h, wavelength λ, and the basic characteristic of the oncoming flow, e.g., δ/λ. Experiments of Sigal[4] and Kendall[5] [$h/\lambda \approx 0(0.03)$] indicate that the wave average friction drag (which, again, is a function of h/λ, δ/λ, etc.) is about 10-20% lower than the flat-plate value. However, the surface pressure distribution is phase-shifted over the wave and produces a form drag; therefore, the total drag of a wavy wall is generally above that of a flat surface. The objective of this portion of the study was to determine whether prescribed distributions of injection/suction on the wavy surface could alter the pressure and skin friction distribution in such a way as to produce a net drag reduction for the surface. The relevant parameters of interest are the peak rate of injection/suction and the distribution of suction/injection with respect to the surface shape, as well as the usual wavy wall flow parameters (h/λ, δ/λ, etc.).

Figure 2 shows a sketch of the surface for which the calculations were made. This surface can be described as

$$y = h\cos(2\pi x\lambda) \qquad (2)$$

The suction distribution at the wall is given by

$$v_w/u_\infty = (v_w/u_\infty)_{\max}\cos(2\pi x/\lambda + \phi) \qquad (3)$$

where ϕ is the phase shift of injection with respect to the surface crest.

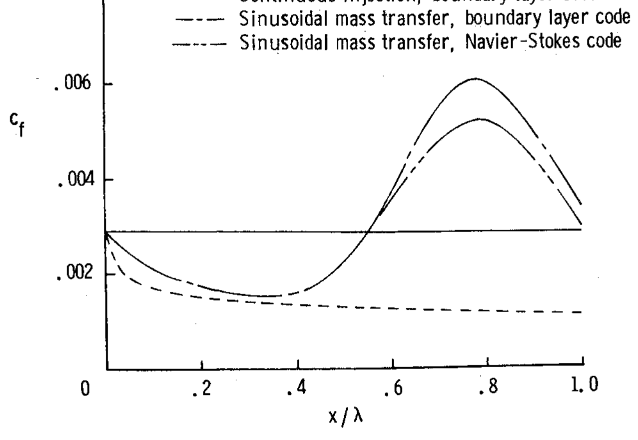

Fig. 1 Local skin friction coefficients calculated by finite difference boundary-layer code and Navier-Stokes code.

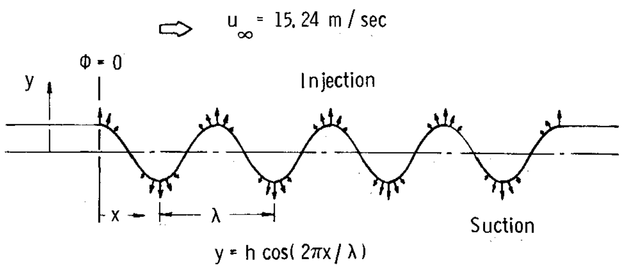

Fig. 2 Sketch of sinusoidal surface illustrating peak injection at crest, peak suction at trough.

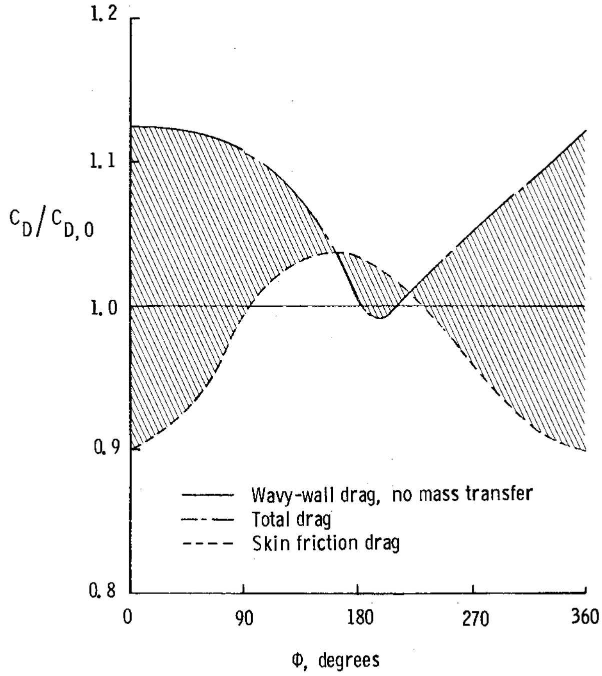

Fig. 3 Effect of phase-shifting sinusoidal mass transfer on the drag of a sinusoidal surface ($\lambda = 30.5$ cm, $h = 0.25$ mm, initial $\delta = 7.6$ cm).

In Fig. 3, the Navier-Stokes calculation for a sinusoidal wave ($h = 0.25$ mm, $\lambda = 30.5$ cm, $\delta = 7.62$ cm) with suction velocity $(v_w/u_\infty)_{\max} = 0.003$ is presented. From the figure it is apparent that at $\phi = 0$ deg a substantial drag penalty is imposed over that of a wavy surface with no mass transfer, mainly through an increase in pressure drag (phase shift). The opposite situation occurs for peak suction at the crest ($\phi = 180$ deg). Here the reduction is mainly due to a pressure thrust. Calculations made with different peak suction rates for the same surface geometry indicate similar trends with ϕ. However, these seems to be a critical $(v_w/u_\infty)_{\max}$ for given wave and flow conditions for which the total drag reduction at $\phi \simeq 180$ deg is a maximum. Above this critical value the total drag goes up for all ϕ. It may thus be possible to obtain a total drag reduction over the wavy surface by a suction distribution with $\phi \simeq 180$ deg. However, the associated penalty for collecting and ducting the flow (which is not considered in this analysis) implies that this is not a desirable option for drag reduction on sine waves.

References

[1]Bushnell, D. M. and Beckwith, I. E., "Calculation of Nonequilibrium Hypersonic Turbulent Boundary Layers and Comparisons with Experimental Data," *AIAA Journal*, Vol. 8, Aug. 1970, pp. 1462-1469.

[2]Balasubramanian, R. and Orszag, S. A., "Numerical Studies of Laminar and Turbulent Drag Reduction," NASA CR 3498, Dec. 1981.

[3]Cebeci, T. and Smith, A.M.O., *Analysis of Turbulent Boundary Layer*, Academic Press, New York, 1974.
[4]Sigal, A., "An Experimental Investigation of the Turbulent Boundary Layer Over a Wavy Wall." Ph.D. Thesis, California University of Technology, Pasadena, Calif., 1971.
[5]Kendall, J. M., "The Turbulent Boundary Layer Over a Wall with Progressive Surface Waves," *Journal of Fluid Mechanics*, Vol. 41, April 1970, p. 259.

Nonunique Solutions to the Transonic Potential Flow Equation

M. D. Salas* and C. R. Gumbert*
NASA Langley Research Center, Hampton, Virginia
E. Turkel†
Institute for Computer Applications in Science and Engineering
NASA Langley Research Center, Hampton, Virginia

Introduction

IN Ref. 1 it was shown that within a certain range of angle of attack α and freestream Mach number M_∞, numerical solutions of the full-potential equation for flow past an airfoil are not unique. The emphasis in Ref. 1 was to show that the anomaly is inherent to the partial-differential equation governing the flow and not a result of its discrete representation. After extensive tests, the authors of Ref. 1 concluded that the nonuniqueness was actually a phenomenon associated with the partial-differential equation. They then conjectured that the anomaly may have a physical basis since it occurred in a range of Mach numbers where airfoils of similar thickness experience buffeting. This, they say, "raises the question of whether an instability of the outer inviscid part of the flow may also be a contributing factor" in the occurrence of buffeting. They suggested that similar investigations using the Euler or Navier-Stokes equations would shed light on the possible physical significance of the observed nonuniqueness. The purpose of this Note is twofold: First, to present results which indicate that the anomaly is due to a breakdown in the potential approximation, rather than a phenomenon associated with the inviscid flowfield; and, second, to show that the lift coefficient C_ℓ, predicted by the potential equation, is a smooth but multivalued function of the angle of attack. This second item fills a gap in the C_ℓ vs α curves presented in Ref. 1; therein, the gap was explained in terms of a hysteresis effect.

Discussion and Results

Parametric studies were conducted in the transonic range for flow past a NACA 0012 airflow using a version of the full-potential multigrid (FL036-2) code described in Ref. 2, the full-potential approximate factorization (TAIR) code described in Ref. 3, and a version of the Euler finite-volume code described in Ref. 4. Table 1 gives the typical grid size and convergence level for each of the codes used in this study. The FL036-2 code included the option of prescribing the lift coefficient and letting the angle of attack which satisfies the Kutta condition evolve as part of the solution. This option had been thoroughly tested and duplicated the results obtained by specifying the angle of attack. Reflection upon the results presented in Ref. 1 indicated that this option was needed to evaluate the C_ℓ vs α curve in the region where C_ℓ is a multivalued function of α.‡ This is the part of the curve which the authors of Ref. 1 failed to generate with α prescribed. Thus, they presented the curve with a gap between its positive- and negative-lift branches. The gap, they argued, was the result of a hysteresis effect. The part of the curve where C_ℓ is a single-valued function of α was obtained here with the TAIR code because of the poor convergence of FL036-2 in this region. The complete curve is shown in Fig. 1 for $M_\infty = 0.83$. Results from all the Euler calculations generated to date and those shown in Fig. 1 do not indicate any anomalous behavior at this Mach number; indeed, the Euler results follow closely the curve predicted by the Prandtl-Glauert thin airfoil approximation,

$$C_\ell = 2\pi\alpha/\sqrt{1-M_\infty^2}$$

The agreement between the Euler solution results and the Prandtl-Glauert theory is fortuitous, since the assumptions on which the latter is based are not valid in the supercritical regime. However, this is not the first instance where Prandtl-

Table 1 Grid size and convergence level for a typical calculation

Code	Mesh (circumf. × radial)	Residual reduced by
TAIR	149 × 30	10^{-6}
FL036-2	192 × 32	10^{-8}
Euler	121 × 35	10^{-6}

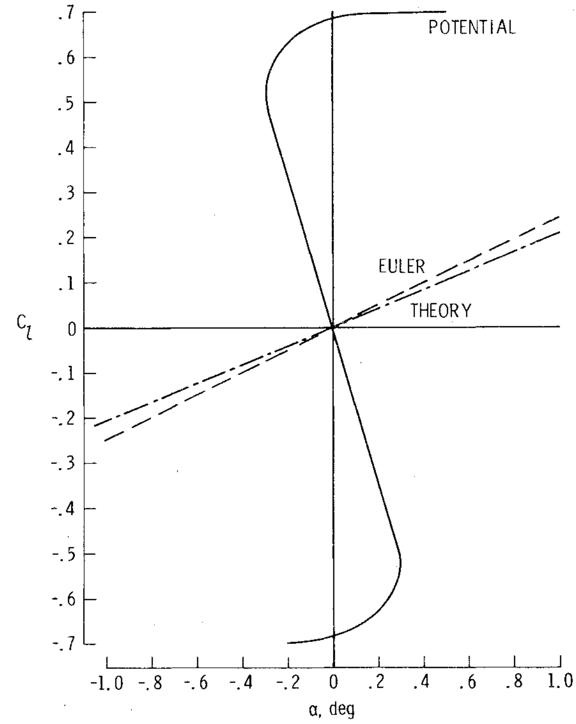

Fig. 1 Lift coefficient as a function of angle of attack computed for an NACA 0012 airfoil at $M_\infty = 0.83$ using FL036-2, TAIR, and an Euler code. The prediction of Prandtl-Glauert theory is included for comparison.

Received Sept. 28, 1982; revision received Dec. 1, 1983. This paper has been declared a work of the U.S. Government and therefore is in the public domain.
*Research Scientist. Member AIAA.
†Visiting Professor, Department of Mathematical Sciences.

‡It has been brought to the authors' attention that R. E. Melnik of Grumman Aerospace Corporation had independently reached the same conclusion and had similarly evaluated this part of the C_ℓ vs α curve.